


# Novel murine model of congenital diabetes: The insulin hyposecretion mouse

Kenta Nakano<sup>1,2</sup>, Rieko Yanobu-Takanashi<sup>2</sup>, Yuki Takahashi<sup>1</sup>, Hayato Sasaki<sup>1</sup>, Yukiko Shimizu<sup>2</sup>, Tadashi Okamura<sup>2,3\*</sup>, Nobuya Sasaki<sup>1\*</sup> 

<sup>1</sup>Laboratory of Laboratory Animal Science and Medicine, School of Veterinary Medicine, Kitasato University, Towada, <sup>2</sup>Department of Laboratory Animal Medicine, and <sup>3</sup>Section of Animal Models, Department of Infectious Diseases, Research Institute, National Center for Global Health and Medicine (NCGM), Tokyo, Japan

## Keywords

Hyperglycemia, Hypoinsulinemia, Non-obese diabetic mouse

## \*Correspondence

Nobuya Sasaki  
Tel.: +81-176-24-9496  
Fax: +81-176-24-9496  
E-mail address:  
nobsasa@vmas.kitasato-u.ac.jp

Tadashi Okamura  
Tel.: +81-3-202-7181 (ext. 2748)  
Fax: +81-3-202-7364  
E-mail address:  
okamurat@ri.ncgm.go.jp

*J Diabetes Investig* 2019; 10: 227–237

doi: 10.1111/jdi.12895

## ABSTRACT

**Aims/Introduction:** Diabetic animal models have made an enormous contribution to our understanding of the etiology of diabetes and the development of new medications. The aim of the present study was to develop and characterize a novel, non-obese murine strain with spontaneous diabetes – the insulin hyposecretion (*ih*s) mouse.

**Materials and Methods:** During the development of the ICGN.B6-*Tns2*<sup>WT</sup> strain as the control for the ICGN-*Tns2*<sup>nph</sup> congenital nephrotic strain, diabetic mice were discovered and named *ih*s mice. Intraperitoneal insulin tolerance test, oral glucose tolerance test and an insulin secretion experiment by the pancreas perfusion system were carried out on *ih*s mice. The pancreatic islets were examined histologically, and the mRNA expression of pancreatic  $\beta$ -cell-specific genes or genes associated with monogenic diabetes was examined by RT-qPCR.

**Results:** The *ih*s mice showed several distinctive diabetes-related characteristics: (i) the onset of diabetes was observed only in the male mice; (ii) there were no differences in insulin content between the *ih*s and control mice; (iii) impaired insulin secretion was elicited by glucose, potassium chloride and sulfonylureas; (iv) there was a significant reduction of relative  $\beta$ -cell volume with no signs of inflammation or fibrosis; (v) they showed a normal glycemic response to exogenous insulin; and (vi) the mice were not obese.

**Conclusions:** The *ih*s mouse provides a novel murine model of congenital diabetes that shows insulin secretion failure. This model allows not only an analysis of the progression of diabetes, but also the identification of unknown genes involved in insulin secretion.

## INTRODUCTION

Type 2 diabetes is a metabolic disorder that is characterized by abnormal glucose homeostasis due to some defect in the secretion and/or action of insulin. There has been a dramatic increase in type 2 diabetes patients in East Asian countries, which now represent one-quarter of the global diabetes population<sup>1</sup>. Although the precise mechanisms that underlie the development and progression of type 2 diabetes have not been fully elucidated, it is thought that a combination of multiple genetic and environmental factors contribute to the pathogenesis of the disease<sup>2</sup>. There has therefore been increased interest in reappraising animal models of type 2 diabetes in which genetic and environmental factors that could influence the development of

the disease and related complications can be precisely controlled *in vivo* to help elucidate the etiology of diabetes and develop new medications. Animal models have made an enormous contribution to the study of diabetes mellitus, providing new information on its management and treatment in humans. Animal models for type 2 diabetes have been widely used for elucidating the genes responsible for the development of type 2 diabetes, the physiological course of the disease and related complications<sup>3,4</sup>.

Type 2 diabetes in East Asian people is characterized by a lower level of obesity compared with type 2 diabetes in Caucasian, as well as a younger age of onset<sup>5,6</sup> and  $\beta$ -cell dysfunction<sup>6–8</sup>. Relatively few people with diabetes in Japan are obese, and the impairment of insulin secretion often develops before the onset of diabetes<sup>9</sup>. Thus, non-obese animal models

Received 10 January 2018; revised 28 June 2018; accepted 1 July 2018

are required to elucidate the complete pathogenesis of diabetes. To this end, we have established a novel, non-obese murine strain with spontaneous diabetes – the insulin hyposecretion (*ih*s) mouse. The *ih*s mouse allows not only the analysis of the progression of diabetes, but also the identification of unknown genes involved in insulin secretion. The present study describes the development and characterization of the *ih*s mouse.

## METHODS

### Ethical statement

All animal experiments were approved by the President of Kitasato University and National Center for Global Health and Medicine, following consideration by the Institutional Animal Care and Use Committee of Kitasato University (approval ID: no. 17-099) and National Center for Global Health and Medicine (approval ID: no. 17056), and were carried out in accordance with institutional procedures, national guidelines and the relevant national laws on the protection of animals.

### Breeding of congenic mice

The ICR-derived glomerulonephritis (ICGN) mouse provides a model of glomerular dysfunction that shows gross morphological changes in the podocyte foot processes that accompany proteinuria (Appendix S1). Previously, we showed that proteinuria in ICGN mice was caused by a deletion mutation in the *tenin2* (*Tns2*) gene (designated *Tns2<sup>np</sup>*)<sup>10,11</sup>. As the original ICGN mouse is a spontaneous mutant derived from closed colony ICR mice, there is no control strain. We therefore created a control strain by using classical breeding methods to introgress the wild-type *Tns2* gene (*Tns2<sup>WT</sup>*) from the C57BL/6J (B6) mouse into the inbred ICGN strain (ICGN.B6-*Tns2<sup>WT</sup>*)<sup>12</sup>. We moved the *Tns2<sup>WT</sup>* allele onto the ICGN genetic background by backcrossing for 10 generations, and subsequently homozygous ICGN.B6-*Tns2<sup>WT</sup>/Tns2<sup>WT</sup>* mice were produced by sib mating. During this strain breeding process, we discovered mutant mice with polydipsia, polyuria, hyperglycemia and hypoinsulinemia, which we named *ih*s mice (Figure 1). As *ih*s mice are spontaneous mutants derived from ICGN mice, which are an animal model for congenital nephrosis, B6 mice were used in the present study as a reference.

### Phenotype measurements

The mice were weighed weekly from 5 weeks-of-age. The nasal-anal length was measured, and the body mass index was calculated at 12, 25 and 52 weeks by taking the weight (g) and dividing it by the square of the nasal-anal length (cm). Body composition was measured by NMR (LF50 BCA-Analyzer; Bruker, Billerica, Massachusetts, USA).

### Blood and urine analysis

Urine glucose levels were measured semiquantitatively using Uro-paper III (Eiken, Tokyo, Japan). To obtain paired

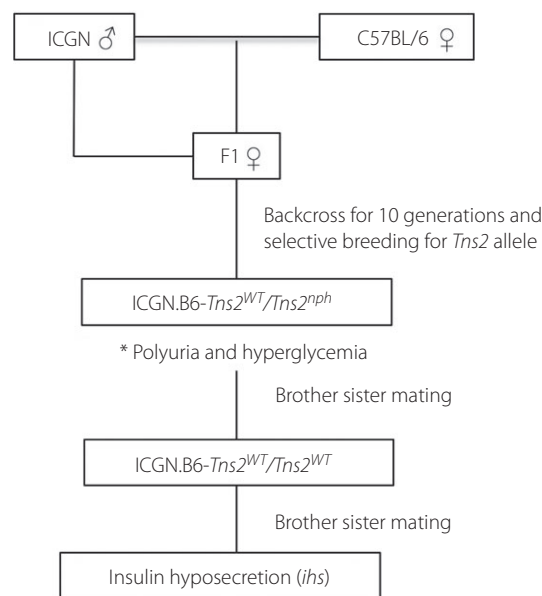


**Figure 1** | The pedigree of insulin hyposecretion (*ih*s) mice developed from ICGN and C57BL/6J mice.

measurements with urine glucose levels, blood was collected by tail snip immediately after urine collection. The blood glucose levels were measured using Glutest Ace and Glutest Sensor (Sanwa Chemical Co., Tokyo, Japan). Diabetes was diagnosed when the glucose level was >250 mg/dL under *ad libitum* feeding conditions.

### Oral glucose and insulin tolerance tests

The mice were fasted for 16 h, and tail blood glucose was measured at 0, 30, 60, 90 and 120 min after the oral administration of glucose (2 g/kg bodyweight; Otsuka Pharmaceutical, Tokyo, Japan) by gavage. Plasma samples were collected from the retro-orbital venous plexus at 0, 15 and 30 min for insulin measurement. Plasma insulin levels were determined by an ultrasensitive mouse insulin kit (Morinaga Institute of Biological Science Inc., Kanagawa, Japan). The area under the curve (AUC) of insulin secretion was calculated after subtraction of the baseline insulin level at the time the glucose was administered.

An insulin tolerance test was carried out after the mice had fasted for 3 h. Insulin (0.75 unit/kg bodyweight; Humulin, Lilly, Indianapolis, Indiana, USA) was injected into the intraperitoneal space, and blood glucose levels were measured with a glucose monitor at 0, 30, 60, 90 and 120 min after the injection.

### Other analyses

Non-fasting plasma insulin and active glucagon-like peptide-1 (GLP-1) levels were measured by enzyme-linked immunosorbent assay (Appendices S2 and S3).

Insulin secretion from *in situ* perfused pancreata (Appendix S4) and insulin secreted by islets isolated from *ihs* mice (Appendix S5) were measured.

Pancreata were subjected to histological analysis, including an analysis of islet morphology, as described previously<sup>13,14</sup>. The details are given in Appendix S6.

RT-qPCR for genes associated with monogenic diabetes was carried out. Details are presented in Appendix S7 and Table S1.

### Statistical analysis

The results are expressed as mean  $\pm$  standard error of the mean. Significant differences in AUC or reverse AUC were analyzed using unpaired Student's *t*-tests. The results for insulin secretion from the *in situ* perfused pancreas analysis were analyzed using repeated-measures ANOVA and Student's *t*-test. Student's *t*-test was used for comparisons of two independent groups, respectively. A *P*-value  $<0.05$  was considered statistically significant.

## RESULTS

### Incidence of diabetes, and survival

The cumulative incidence of diabetes in *ihs* mice, determined by the casual blood glucose level, is shown in Figure 2a. Diabetes was observed only in male mice. The earliest onset was observed at 9–12 weeks, and its incidence increased with age (33 and 89% at 12 and 42 weeks, respectively). Glucosuria appeared in male mice at 9–12 weeks, concomitant with the onset of diabetes, and was present in 88.9% of mice aged 42 weeks (Figure 2b). Because the onset of diabetes differed between the sexes, we focused our studies on male mice. At 45 weeks-of-age, the survival rate of the male *ihs* mice was approximately 50%, decreasing to approximately 42% at 51 weeks, compared with 81% survival at 51 weeks in female *ihs* mice (Figure 2c). This indicated that the onset of diabetes influenced the survival of male *ihs* mice.

### Clinical features of the *ihs* mice

Aged 11 weeks, the *ihs* mice ( $32.4 \pm 0.4$  g,  $n = 10$ ) were significantly lighter than the ICR mice ( $33.8 \pm 1.9$  g,  $P < 0.01$ ,  $n = 9$ ). However, at 12 weeks, the *ihs* mice were heavier than the B6 strain mice (Figure 3a). The bodyweight of the B6 mice continued to increase until 52 weeks-of-age, whereas growth in the *ihs* mice reached a plateau (35 g) at 25 weeks (Figure 3b), with their weight gradually decreasing to approximately 61% of that of B6 mice at 52 weeks. A significant decrease in body weight was observed after the onset of diabetes. The two strains of mice had similar body mass index values at 25 weeks (Figure 3c), indicating that the *ihs* mice were non-obese. The analysis of body composition using the NMR method showed that the relative fat percentage was significantly lower in *ihs* mice, being approximately 47 and 20% of that of B6 mice at 25 and 52 weeks-of-age, respectively, with a concomitant increase in lean mass (Figure 3d). These findings showed that the bodyweight reduction in

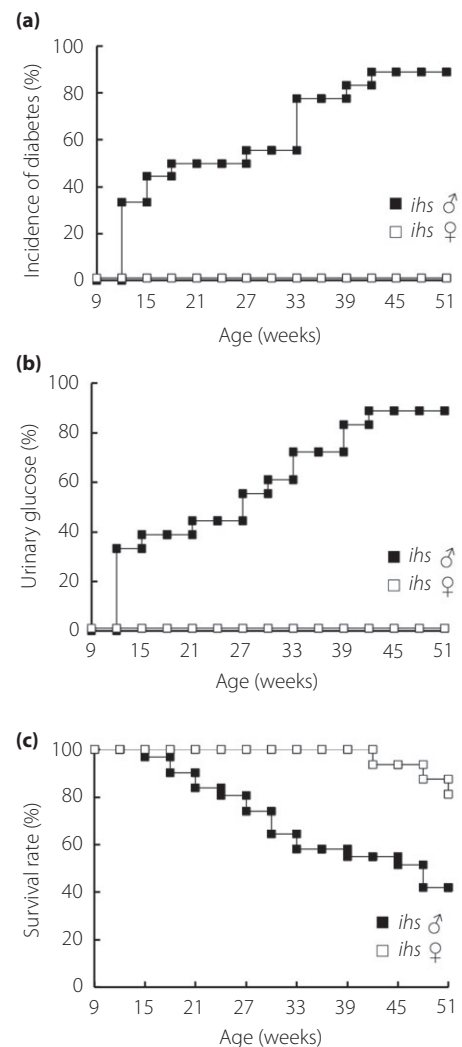


**Figure 2** | The incidence of diabetes and the rate of survival in *ihs* mice. (a,b) The cumulative incidence of diabetes in *ihs* male ( $n = 18$ ) and female ( $n = 16$ ) mice. Diabetes is defined as a blood glucose level of  $\geq 250$  mg/dL under *ad libitum* feeding conditions. (c) Cumulative survival rate of *ihs* mice. The cumulative survival rate was plotted against age in weeks ( $n = 31$  and 16 mice for male and female mice, respectively).

*ihs* mice was largely due to decreased fat mass, thought to be associated with the onset of diabetes.

To assess whether the *ihs* mice were hyperphagic, the daily food intake was monitored in animals fed a standard chow diet *ad libitum*. At 12 and 25 weeks, the *ihs* mice consumed approximately 50% more food than the controls, indicating marked hyperphagia (Figure 3e). In addition, a significant increase ( $P < 0.05$ ) in total water intake was observed in *ihs* mice throughout the experimental period (Figure 3f). However, no proteinuria was observed and there were no obvious pathological changes in the glomeruli at 45 weeks-of-age in the male *ihs* mice (data not shown).

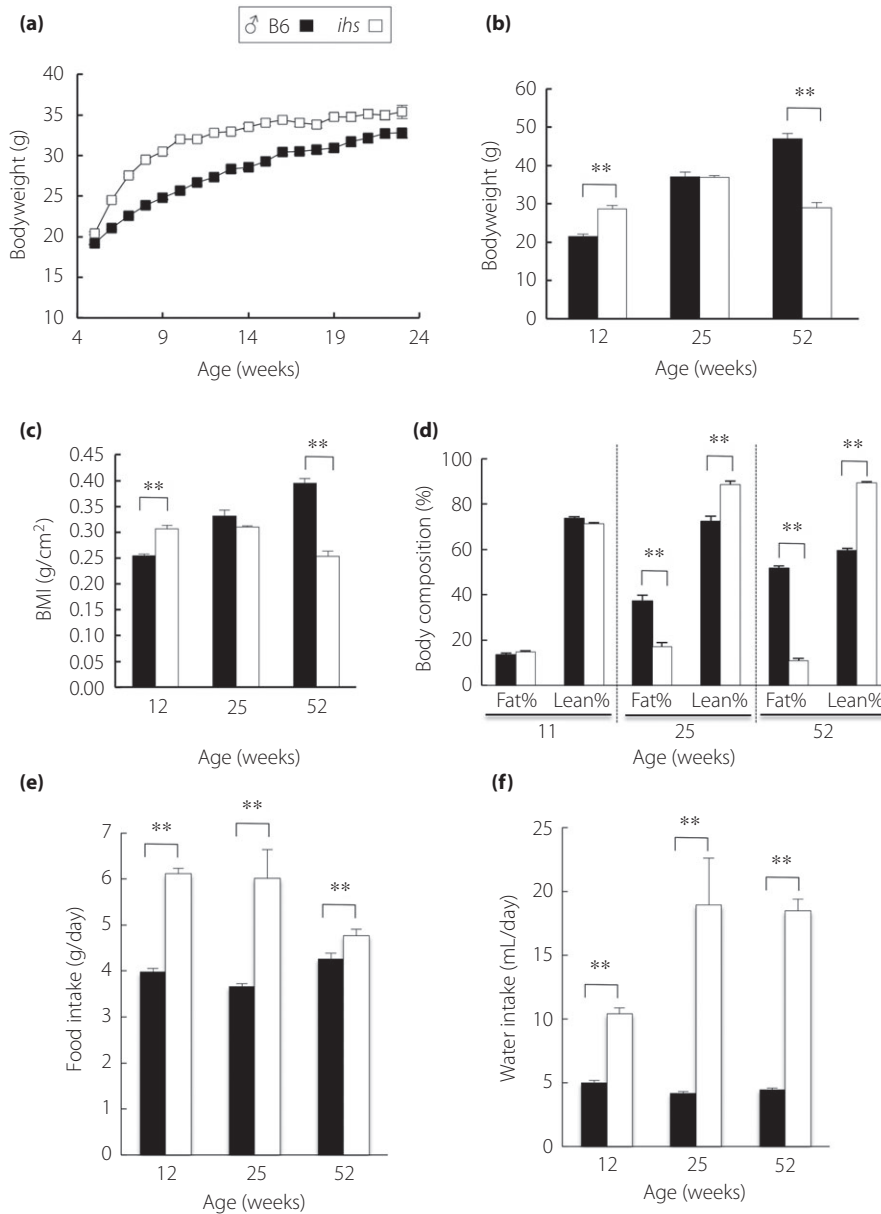


**Figure 3** | Bodyweight, body mass index (BMI), body composition, water consumption and food intake in *ihs* mice. (a) Change in bodyweight in male *ihs* ( $n = 8$ ) and B6 ( $n = 10$ ). (b,c) Bodyweight in male *ihs* ( $n = 4$ ) and B6 mice ( $n = 5$ ) was measured at the indicated ages. BMI was calculated as bodyweight (g) divided by the square of the anal-nasal length (cm<sup>2</sup>) at the indicated ages. (d) Comparison of body composition at the indicated ages. (e,f) Water consumption and mean daily food intake were measured at the indicated ages. Data were analyzed by Student's *t*-test (\*\* $p < 0.01$ , *ihs* mice vs age-matched B6).

### Glucose tolerance and insulin response to oral glucose loading and sensitivity to insulin

To characterize the *ihs* mice in terms of systemic glucose homeostasis and insulin release *in vivo*, we carried out oral glucose tolerance tests (OGTTs) on *ihs* and control mice. At 10 weeks-of-age, there was no difference in fasting glucose levels between the *ihs* and control animals, but the male *ihs* mice showed typical glucose levels of  $\geq 300$  mg/dL, typical of diabetes, at 30–120 min

after glucose loading (Figure 4a). Although the female *ihs* mice showed normal blood glucose levels in the non-fasting state, they showed marked impairment in glucose tolerance (Figure 4b). The glucose AUC values after glucose loading in male and female *ihs* mice were significantly higher than those in B6 mice. Impaired glucose tolerance was observed in all male and female *ihs* mice with an exacerbation of glucose tolerance in an age-dependent manner (Figure S1a,b).

Insulin concentrations were also measured during the OGTTs. The non-fasting insulin levels (Figure S2) and the plasma insulin levels of the *ihs* and control mice before glucose administration were similar (Figure 4c,d). After glucose loading, the *ihs* mice showed significantly lower insulin levels and the insulin AUC values were also lower (Figure 4c,d). This suggested that *ihs* mice have defective glucose-stimulated insulin secretion at the early phase of diabetes. Insulin release *in vivo* during the OGTTs was markedly impaired in male and female *ihs* mice, resulting in marked impairment in glucose tolerance. The plasma GLP-1 levels after glucose loading in *ihs* mice was comparable with that of the control mice (Figure S3).

To test for insulin sensitivity, we carried out insulin tolerance tests on *ihs* and control mice (Figure 4e,f). The *ihs* mice showed a normal glycemic response to exogenous insulin and were not insulin-resistant.

#### Histological examination of pancreatic islets in male *ihs* mice

Islets from mutant and control mice at 10–12 weeks-of-age were of similar size and shape with a smooth periphery (Figure 5a). No inflammation or fibroblast proliferation was observed in the mutant mouse islets. Immunostaining for insulin showed that insulin-positive cells were regularly distributed. Furthermore, no differences in pancreatic insulin contents were observed between the mutant and control mice (Figure 5b), and the sizes of individual  $\beta$ -cells from the histological sections were similar in the mutant and control mice (Figure 5c). Next, the volume of  $\beta$ -cells relative to the gross volume of the pancreas was determined to analyze sections that were immunostained for insulin. In male *ihs* mice, the relative  $\beta$ -cell volume was significantly lower than that in the control B6 mice (Figure 5d), and the ratio of  $\alpha/\beta$ -cells in the *ihs* islets was significantly increased (Figure 5e). In aged male and female *ihs* mice, the increase in  $\alpha$ -cells was more pronounced (Figures S4 and S5); a marked decrease in the number of islets was observed only in aged male *ihs* mice. In mouse islets under normal conditions,  $\alpha$ -cells are localized in the islet periphery. However, the pattern of peripheral distribution of  $\alpha$ -cells seemed to be disrupted, and some  $\alpha$ -cells were scattered throughout the islet core in the pancreas of *ihs* mice in a manner similar to that observed in diabetes models (Figure 5a)<sup>15</sup>.

#### Insulin secretion from perfused pancreata and isolated islets

We hypothesized that abnormal insulin secretion was the cause of the hypoinsulinemic hyperglycemia in the *ihs* mice. To test this, we carried out perfusion experiments that examined the time-course of the insulin secretory response to high glucose. In the control pancreata, a change in glucose concentration from 2.8 to 16.5 mmol/L elicited strong peaks, with a 14-fold increase in insulin secretion (Figure 6a). As was expected from the results of the OGTTs, the elevation of glucose concentration from 2.8 to 16.5 mmol/L in the pancreata of the *ihs* mice resulted in a fourfold increase in insulin secretion. In the *ihs* mice, the AUC values of secreted insulin after glucose

stimulation (from 10 to 26 min) was significantly impaired compared with that of the control mice ( $24.5 \pm 9$  vs  $92.4 \pm 13.1$ ;  $P < 0.01$ ; Figure 6b).

Islet  $\beta$ -cell glucose metabolism is accompanied by closure of the adenosine triphosphate-sensitive potassium channels followed by depolarization. We therefore investigated insulin secretion in response to potassium chloride (KCl), a potent insulin secretagogue, to identify which steps in the insulin secretion pathway are impaired in *ihs* mice. The *ihs* pancreata showed a significantly lower increase in insulin secretion compared with the control pancreata (an 8-fold increase vs a 47-fold increase;  $P < 0.05$ ; Figure 6a), indicating a significant reduction in insulin secretion in the *ihs* mice (Figure 6b). In the batch incubation experiment, the islets isolated from *ihs* mice also showed a significant decrease in insulin secretion compared with those isolated from control mice, when stimulated with glibenclamide, (antidiabetic drug of class sulfonylureas), which causes the  $\beta$ -cell depolarization (Figure S6)<sup>16</sup>. These results showed that the insulin secretion capability of  $\beta$ -cells was markedly impaired in *ihs* mice.

#### Assessment of pancreatic $\beta$ -cell gene expression in the islets of *ihs* and control mice

Glucose-stimulated insulin secretion can be impaired after a reduction in the proteins involved in glucose sensing and insulin secretion. To determine whether the defect in insulin secretion in *ihs* mice was associated with abnormalities in gene transcription, the expression of pancreatic  $\beta$ -cell-specific genes or genes associated with monogenic diabetes was assessed by RT-qPCR (Figure 7). Most of these genes showed no change in expression in comparison with control mice. However, *Glp1r* was significantly upregulated, and the expression levels of *Glis3*, *Glut2*, *Wfs1* and *Epac2* were downregulated, in the islets of the *ihs* mice.

#### DISCUSSION

Animal models of diabetes that more closely recapitulate the features of the human disease would be useful for understanding the pathogenesis and developing new treatment strategies. The *ihs* mice showed several distinctive diabetes-related characteristics: (i) the onset of diabetes was observed only in the male mice; (ii) there were no differences in insulin content between the *ihs* and control mice; (iii) impaired insulin secretion was elicited by glucose and KCl; (iv) there was a significant reduction of relative  $\beta$ -cell volume with no signs of inflammation or fibrosis; (v) they showed a normal glycemic response to exogenous insulin; and (vi) they were non-obese. Nagoya–Shibata–Yasuda (NSY) mice, a type 2 diabetes model derived from ICR mice, showed phenotypes similar to that of *ihs* mice, such as severely impaired glucose tolerance, reduction in glucose-stimulated insulin secretion and differences in diabetes onset based on sex<sup>17–20</sup>. However, NSY mice showed an increase in the fasting plasma insulin levels, insulin resistance and hypertrophy of pancreatic islets, whereas *ihs* mice had normal fasting plasma



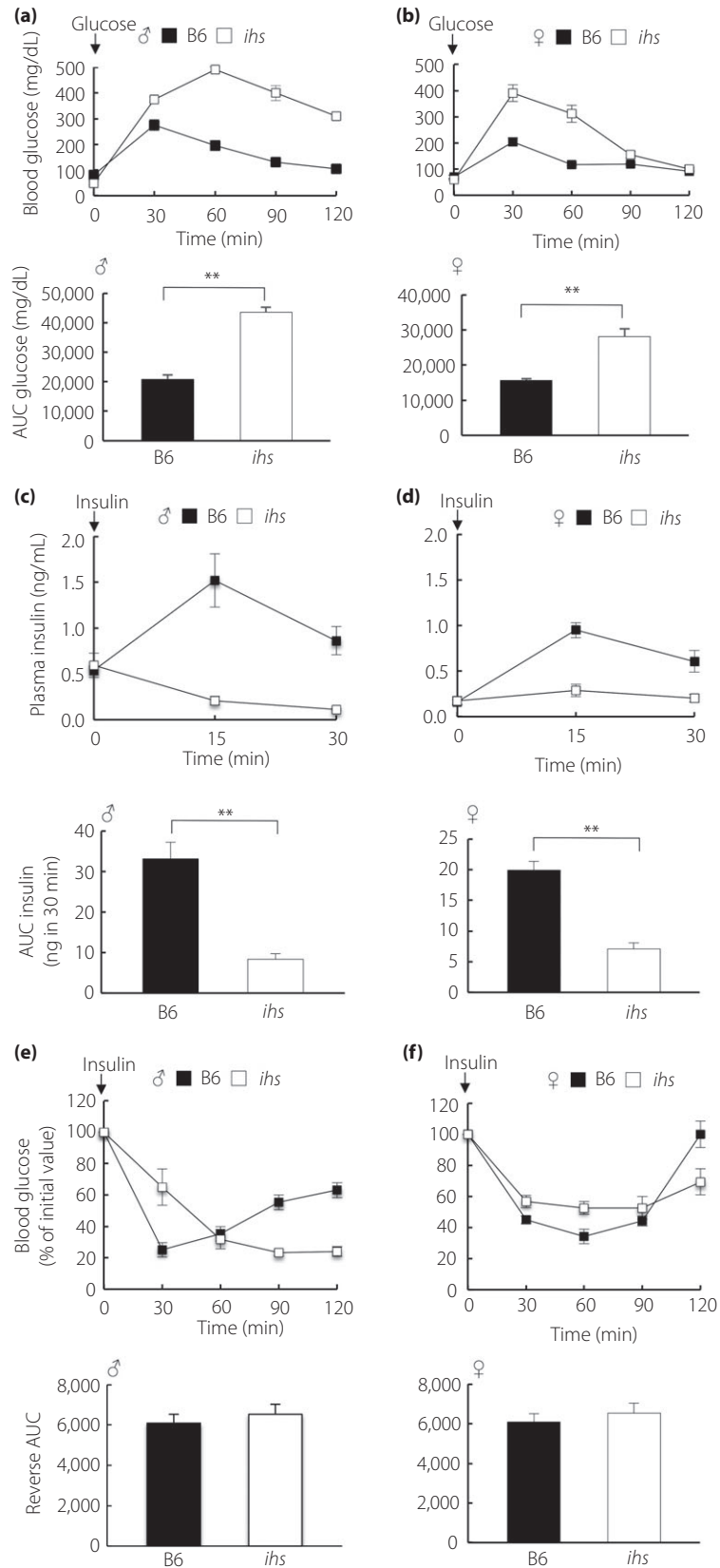


**Figure 4** | Glucose tolerance, insulin secretion and insulin sensitivity in *ihs* mice. (a,b) Upper figure: oral glucose tolerance test (2 g/kg) at 10–12 weeks-of-age in male B6 ( $n = 5$ ) and *ihs* ( $n = 5$ ) mice, and in female B6 ( $n = 6$ ) and *ihs* ( $n = 5$ ) mice. Blood glucose was measured at 0, 30, 60, 90 and 120 min in response to oral glucose administration in 16 h-fasted mice. Lower figure: the area under the curve (AUC) of the 0–120 min glycemic responses.  $AUC_{\text{glucose}}$  was calculated using the trapezoidal rule. Data were analyzed by Student's *t*-test (\*\* $P < 0.01$ , *ihs* mice vs pair-fed B6). (c,d) Upper figure: plasma insulin concentrations during the oral glucose tolerance tests (2 g/kg) at 10–12 weeks-of-age in male B6 ( $n = 5$ ) and *ihs* ( $n = 4$ ) mice, and in female B6 ( $n = 6$ ) and *ihs* ( $n = 5$ ) mice. Plasma insulin was measured at 0, 15 and 30 min in response to oral glucose administration in 16 h-fasted mice. Lower figure:  $AUC_{\text{insulin}}$  of the 0–30 min % of initial value was calculated using the trapezoidal rule. Data were analyzed by Student's *t*-test (\*\* $P < 0.01$ , *ihs* mice vs age-matched B6). (e,f) Blood glucose (% of initial value) during the insulin tolerance test (0.75 IU/kg) at 10–12 weeks-of-age in male B6 ( $n = 6$ ) and *ihs* ( $n = 8$ ) mice, and in female B6 ( $n = 7$ ) and *ihs* ( $n = 7$ ) mice. The reverse AUC was calculated using the trapezoidal rule. Data were analyzed by Student's *t*-test.

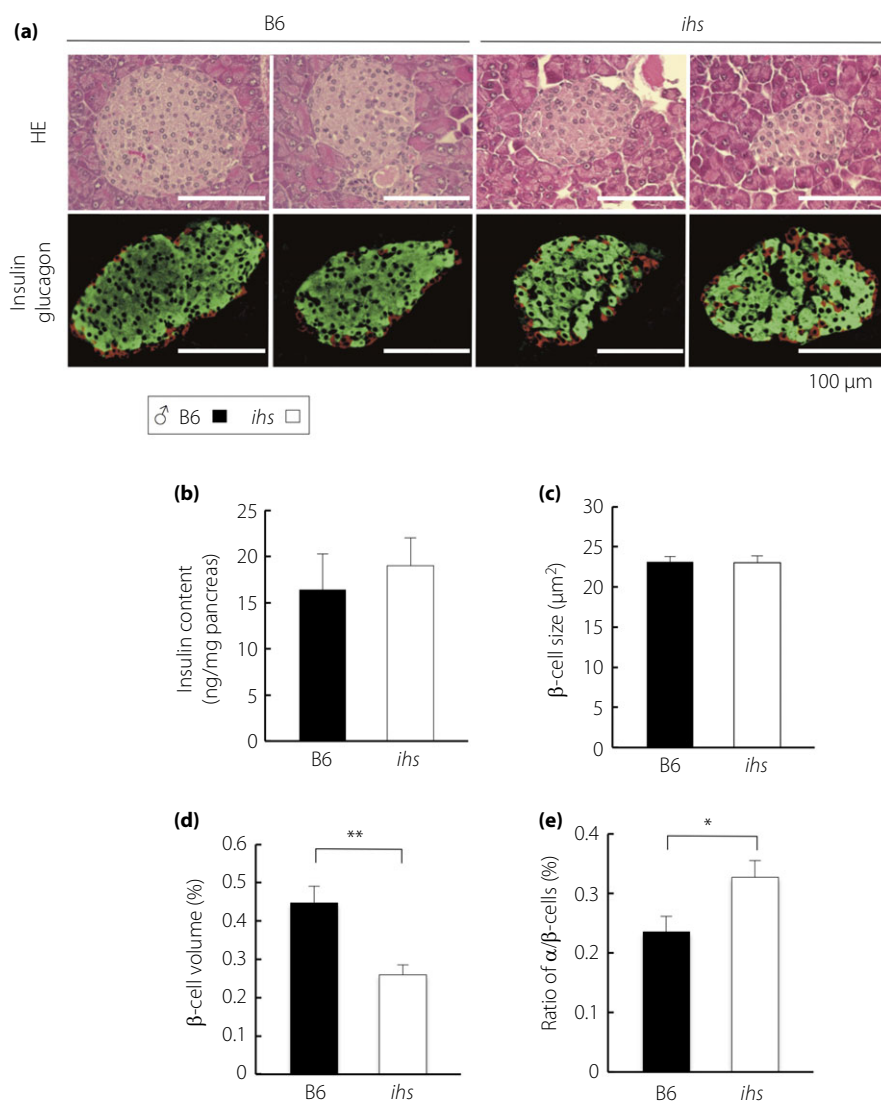


**Figure 5** | Pancreatic islet morphology. (a) Upper panels: pancreatic histological sections of male B6 and *ihs* mice at 10–12 weeks-of-age stained with hematoxylin–eosin (HE). Lower panels: immunohistochemistry with antibodies against insulin (green) and glucagon (red). (b) Insulin content, (c)  $\beta$ -cell size, (d) Relative  $\beta$ -cell volume (%) and (e) the ratio of  $\alpha$ - to  $\beta$ -cell areas in the pancreas ( $\alpha/\beta$ -ratio). B6 ( $n = 3$ ) and *ihs* ( $n = 3$ ) mice. Data were analyzed by Student's *t*-test (\* $P < 0.05$ , \*\* $P < 0.01$ ). Scale bar, 100  $\mu\text{m}$ .

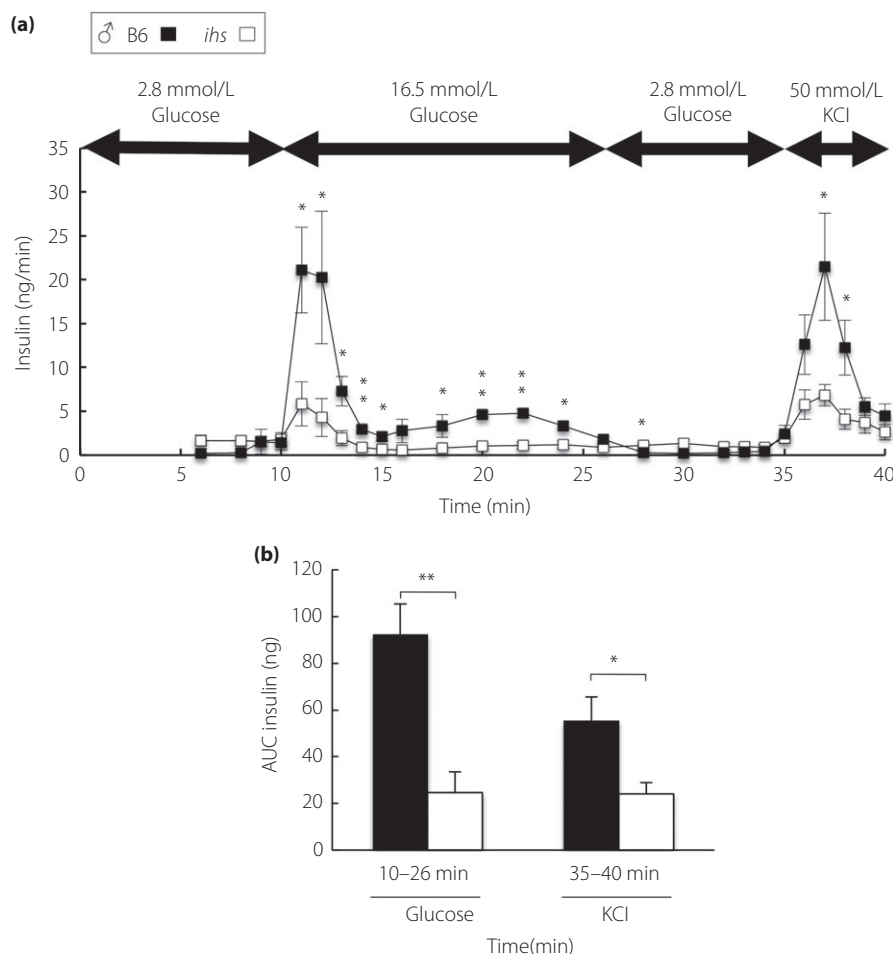


**Figure 6** | Insulin secretion of perfused pancreata in response to high glucose and potassium chloride (KCl). (a) After a baseline period (10 min), glucose concentration in perfusate was shifted from 2.8 to 16.7 mmol/L for 15 min, and was then reduced to 2.8 mmol/L for 5 min, and 50 mmol/L KCl was then added to the perfusate. The amounts of secreted insulin in B6 (closed square,  $n = 4$ ) and *ihs* (open square,  $n = 6$ ) mice after stimulation with 16.7 mmol/L glucose and KCl are expressed as the area under the curve for insulin ( $AUC_{\text{insulin}}$ ) from 10 to 26 min and 35 to 40 min, respectively. (b) The AUCs were assessed for insulin levels in the perfusate ( $AUC_{\text{insulin}}$ ) using the trapezoidal rule of suprabasal values. Data were analyzed by Student's *t*-test (\* $P < 0.05$ , \*\* $P < 0.01$ ).

insulin levels and insulin sensitivity, and showed the relative  $\beta$ -cell volume was lower than that in control mice. Furthermore, the incidence of diabetes in the female NSY mice was 31% at 48 weeks, whereas the female *ihs* mice did not develop diabetes, although female *ihs* mice have impaired glucose tolerance. Therefore, we concluded that the *ihs* mouse was a novel murine model for non-obese type 2 diabetes.

The release of insulin from pancreatic  $\beta$ -cells is regulated by highly complex and sophisticated mechanisms, modulated by many factors, including hormones, neuropeptides and neurotransmitters<sup>21</sup>. With respect to the mechanism in  $\beta$ -cells, we showed that *Glut2*, *Wfs1* and *Epac2* expression levels were significantly downregulated (by 50%) in the islets of the *ihs* mice, and that *Glp1r* expression was increased threefold. The GLP-1 receptor (GLP1R) is expressed mainly in the alimentary tract,

particularly in the pancreatic islet cells<sup>22</sup>, where it mediates the actions of GLP-1 released from the small intestines in response to food intake. GLP-1 is considered to be one of the most important glucose-dependent insulin secretagogues<sup>23</sup>, and is known to cause a rise in intracellular  $Ca^{2+}$  concentration<sup>24</sup>. The GLP1R, a G-protein-coupled receptor, is involved in insulin secretion through mechanisms dependent on and independent of PKA<sup>25</sup>. GLP-1 stimulates the expression of glucose transporter 2, which determines the rate of glycolysis and helps to confer the glucose competence to  $\beta$ -cells, thereby increasing the efficacy and potency of glucose as a stimulus for insulin secretion<sup>25</sup>. It has been reported that WFS1 is essential for GLP-1-stimulated cAMP production, and the regulation of insulin biosynthesis and secretion<sup>26</sup>. In pancreatic  $\beta$ -cells, cAMP signaling, which can be activated by various extracellular stimuli,



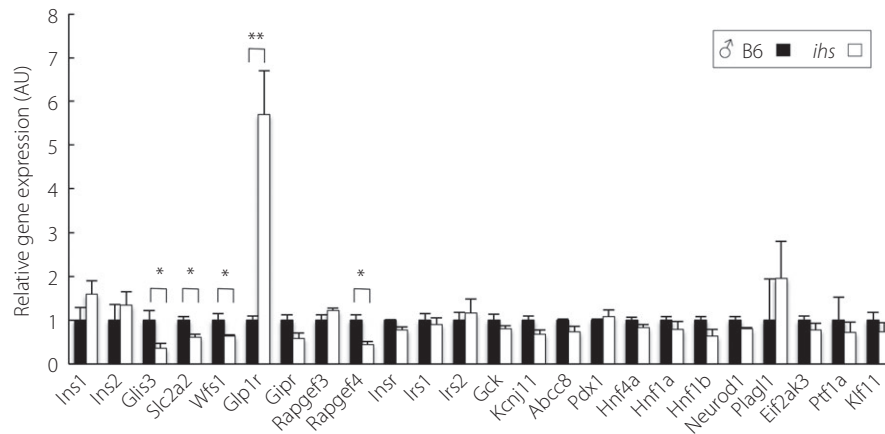


**Figure 7** | Comparison of the expression of diabetes-related genes between islets from B6 and *ihs* mice. RT-qPCR analysis of diabetes-related genes for isolated *ihs* islets at 10 weeks-of-age. The values were arbitrary units after normalization against *Actb*. All data are expressed as mean  $\pm$  standard error of the mean, and data were analyzed by Student's *t*-test (\* $P < 0.05$ , \*\* $P < 0.01$ ). B6 ( $n = 3$ ) and *ihs* ( $n = 3$ ) mice. Each experiment was carried out in three biological replicates.

including hormonal and neural inputs primarily through G-protein-coupled receptors, is vital for the normal regulation of insulin secretion to maintain glucose homeostasis. The activation of cAMP signaling amplifies insulin secretion dependent on exchange protein directly activated by cAMP 2 (EPAC2)<sup>27</sup>. EPAC2 is essential in the potentiation of insulin granule exocytosis by cAMP, primarily in the first phase of cAMP-potentiated exocytosis, by increasing the number of restless newcomers<sup>27</sup>. Although the plasma GLP-1 concentration was comparable with the control mouse (Figure S3), the unresponsiveness of the pathway induced by GLP1R activation might cause the upregulation of *Glp1r*, and downregulation of *Glut2*, *Wfs1* and *Epac2* expression in the *ihs* mouse.

A high concentration of KCl and sulfonylureas can directly cause depolarization of the  $\beta$ -cell plasma membrane, which subsequently triggers an influx of  $\text{Ca}^{2+}$  and insulin granule exocytosis<sup>16,28</sup>. This indicates that the defective insulin release induced by KCl in the perfusion experiments (Figure 6) and by glibenclamide in batch incubation experiments (Figure S6) was not caused by a defect in GLP-1 signaling. The causative gene for insulin hyposecretion in the *ihs* mouse is not involved in incretin-potentiated insulin secretion. However, the GLP-1 signal elevates cytosolic  $\text{Ca}^{2+}$  in  $\beta$ -cells<sup>24,29</sup>. Thus, the significant upregulation of *Glp1r* and marked impairment of insulin secretion stimulated by glucose and KCl might be caused by a defect in the  $\text{Ca}^{2+}$  signaling pathway in the  $\beta$ -cells of the *ihs* mice. Although relative  $\beta$ -cell volume of *ihs* mice decreased to almost 60% of that of the B6 mice (Figure 5d), no differences were observed in the insulin content of the pancreata and in the  $\beta$ -cell size between the *ihs* and control mice (Figure 5b,c), and insulin 1 and 2 mRNA levels were similar in the two strains (Figure 6). This suggests the possibility that more insulin granules are stocked in each  $\beta$ -cell of *ihs* mice. Therefore, we

concluded that the marked dysfunction in insulin secretion observed in the *ihs* mice at a young age was not caused by a defect in the insulin production or islet architecture and organization, but by a defect in the  $\text{Ca}^{2+}$  influx and/or  $\text{Ca}^{2+}$  signaling pathway in  $\beta$ -cells.

The incidence of diabetes in the male *ihs* mice was 90% at 42 weeks-of-age; in contrast, none of the female mice developed diabetes, even though the female *ihs* mice showed impaired glucose tolerance and the impairment of glucose-induced insulin secretion (Figures 4b,d and S1b). In the present study, we found that the relative  $\beta$ -cell volume in the male *ihs* mice was lower than that in age-matched B6 mice (Figure 5d), and progressively decreased with aging (Figure S4). In contrast, marked reduction of islets was not observed in aged female *ihs* mice (Figure S5). It seemed that the reduction of islets in aged male *ihs* mice was influenced by glucotoxicity. Additionally, glucagon-positive  $\alpha$ -cells were evenly distributed along the periphery of the islets in the control mice. However, a relative increase in  $\alpha$ -cells along the periphery and in the central core of the islet was more evident with aging in the male and female *ihs* mice (Figures S4 and S5). A relative increase in  $\alpha$ -cells has been reported in many animal models with  $\beta$ -cell deficiency<sup>15</sup>, as well as in patients with type 2 diabetes<sup>30,31</sup>. This is thought to result from the collapse of the central  $\beta$ -cell core due to the loss of  $\beta$ -cells rather than from  $\alpha$ -cell hyperplasia. A similar sex difference has been observed in a variety of diabetic cases in humans<sup>32,33</sup>. In addition, many knock-out and transgenic models of diabetes show a sex bias<sup>34</sup>, and the protective effect of estradiol against the development of insulin resistance and diabetes has been widely discussed<sup>35,36</sup>. We assume that estrogen and prolactin play a protective role in female rodents, as they have a regulatory influence on  $\beta$ -cell function<sup>37</sup> and proliferation rates<sup>38</sup>. Further research is warranted to elucidate the mechanism(s) underlying this sex bias.

Models of spontaneous diabetes are invaluable for the identification of unknown diabetogenic genes. The *ihs* mouse model involves neither obesity nor insulinitis, but is accompanied by notable pancreatic  $\beta$ -cell dysfunction, which distinguishes it from other well-characterized animal models. Although further genetic analysis is required to allow a better understanding of the molecular pathology of *ihs* mice, our preliminary exome sequencing analysis from ICGN mice and genetic analysis in *ihs* mice showed no non-synonymous, nonsense or frameshift mutations in the known genes responsible for monogenic diabetes characterized by  $\beta$ -cell failure in humans and rodents. This suggests that the *ihs* strain can contribute to the discovery of novel causative genes, potentially leading to the development of treatment strategies for hypoinsulinemia and diabetes.

### ACKNOWLEDGMENTS

This work was supported by the Ministry of Education, Culture, Sports, Science and Technology (MEXT); Grants-in-Aid for Scientific Research, KAKENHI (16K07094 and 26430101) to NS and TO, and was partially supported by Grants-in-Aid for Research from the National Center for Global Health and Medicine (26-105 and 29-1001).

### DISCLOSURE

The authors declare no conflict of interest.

### REFERENCES

1. Yabe D, Seino Y, Fukushima M, *et al.* beta cell dysfunction versus insulin resistance in the pathogenesis of type 2 diabetes in East Asians. *Curr Diab Rep* 2015; 15: 602.
2. O'Rahilly S, Barroso I, Wareham NJ. Genetic factors in type 2 diabetes: the end of the beginning? *Science* 2005; 307: 370–373.
3. Al-Awar A, Kupai K, Veszelka M, *et al.* Experimental diabetes mellitus in different animal models. *J Diabetes Res* 2016; 2016: 9051426.
4. Kitada M, Ogura Y, Koya D. Rodent models of diabetic nephropathy: their utility and limitations. *Int J Nephrol Renovasc Dis* 2016; 9: 279–290.
5. Yoon KH, Lee JH, Kim JW, *et al.* Epidemic obesity and type 2 diabetes in Asia. *Lancet* 2006; 368: 1681–1688.
6. Moller JB, Pedersen M, Tanaka H, *et al.* Body composition is the main determinant for the difference in type 2 diabetes pathophysiology between Japanese and Caucasians. *Diabetes Care* 2014; 37: 796–804.
7. Moller JB, Dalla Man C, Overgaard RV, *et al.* Ethnic differences in insulin sensitivity, beta-cell function, and hepatic extraction between Japanese and Caucasians: a minimal model analysis. *J Clin Endocrinol Metab* 2014; 99: 4273–4280.
8. Fukushima M, Suzuki H, Seino Y. Insulin secretion capacity in the development from normal glucose tolerance to type 2 diabetes. *Diabetes Res Clin Pract* 2004; 66: S37–S43.
9. Gerich JE. Metabolic abnormalities in impaired glucose tolerance. *Metabolism* 1997; 46: 40–43.
10. Cho AR, Uchio-Yamada K, Torigai T, *et al.* Deficiency of the *tensin2* gene in the ICGN mouse: an animal model for congenital nephrotic syndrome. *Mamm Genome* 2006; 17: 407–416.
11. Marusugi K, Nakano K, Sasaki H, *et al.* Functional validation of *tensin2* SH2-PTB domain by CRISPR/Cas9-mediated genome editing. *J Vet Med Sci* 2016; 78: 1413–1420.
12. Sasaki H, Kimura J, Nagasaki K, *et al.* Mouse chromosome 2 harbors genetic determinants of resistance to podocyte injury and renal tubulointerstitial fibrosis. *BMC Genet* 2016; 17: 69.
13. Frantz ED, Aguila MB, Pinheiro-Mulder Ada R, *et al.* Transgenerational endocrine pancreatic adaptation in mice from maternal protein restriction *in utero*. *Mech Ageing Dev* 2011; 132: 110–116.
14. Bernal-Mizrachi E, Wen W, Stahlhut S, *et al.* Islet beta cell expression of constitutively active Akt1/PKB alpha induces striking hypertrophy, hyperplasia, and hyperinsulinemia. *J Clin Invest* 2001; 108: 1631–1638.
15. Kharouta M, Miller K, Kim A, *et al.* No mantle formation in rodent islets – the prototype of islet revisited. *Diabetes Res Clin Pract* 2009; 85: 252–257.
16. Fuhendorff J, Rorsman P, Kofod H, *et al.* Stimulation of insulin release by repaglinide and glibenclamide involves both common and distinct processes. *Diabetes* 1998; 47: 345–351.
17. Shibata M, Yasuda B. New experimental congenital diabetic mice (N.S.Y. mice). *Tohoku J Exp Med* 1980; 130: 139–142.
18. Ueda H, Ikegami H, Yamato E, *et al.* The NSY mouse: a new animal model of spontaneous NIDDM with moderate obesity. *Diabetologia* 1995; 38: 503–508.
19. Ueda H, Ikegami H, Kawaguchi Y, *et al.* Age-dependent changes in phenotypes and candidate gene analysis in a polygenic animal model of Type II diabetes mellitus. *NSY mouse*. *Diabetologia* 2000; 43: 932–938.
20. Hamada Y, Ikegami H, Ueda H, *et al.* Insulin secretion to glucose as well as nonglucose stimuli is impaired in spontaneously diabetic Nagoya-Shibata-Yasuda mice. *Metabolism* 2001; 50: 1282–1285.
21. Roder PV, Wu B, Liu Y, *et al.* Pancreatic regulation of glucose homeostasis. *Exp Mol Med* 2016; 48: e219.
22. Wei Y, Mojsov S. Tissue-specific expression of the human receptor for glucagon-like peptide-I: brain, heart and pancreatic forms have the same deduced amino acid sequences. *FEBS Lett* 1995; 358: 219–224.
23. Vella A, Cobelli C. Defective glucagon-like peptide 1 secretion in prediabetes and type 2 diabetes is influenced by weight and sex. Chicken, egg, or none of the above? *Diabetes* 2015; 64: 2324–2325.
24. Yada T, Itoh K, Nakata M. Glucagon-like peptide-1-(7-36) amide and a rise in cyclic adenosine 3',5'-monophosphate increase cytosolic free  $Ca^{2+}$  in rat pancreatic beta-cells by

- enhancing Ca<sup>2+</sup> channel activity. *Endocrinology* 1993; 133: 1685–1692.
25. Doyle ME, Egan JM. Glucagon-like peptide-1. *Recent Prog Horm Res* 2001; 56: 377–399.
  26. Lemaire K, Schuit F. Integrating insulin secretion and ER stress in pancreatic beta-cells. *Nat Cell Biol* 2012; 14: 979–981.
  27. Almahariq M, Mei FC, Cheng X. Cyclic AMP sensor EPAC proteins and energy homeostasis. *Trends Endocrinol Metab* 2014; 25: 60–71.
  28. Gilon P, Chae HY, Rutter GA, *et al.* Calcium signaling in pancreatic beta-cells in health and in type 2 diabetes. *Cell Calcium* 2014; 56: 340–361.
  29. Bode HP, Moormann B, Dabew R, *et al.* Glucagon-like peptide 1 elevates cytosolic calcium in pancreatic beta-cells independently of protein kinase A. *Endocrinology* 1999; 140: 3919–3927.
  30. Henquin JC, Rahier J. Pancreatic alpha cell mass in European subjects with type 2 diabetes. *Diabetologia* 2011; 54: 1720–1725.
  31. Yoon KH, Ko SH, Cho JH, *et al.* Selective beta-cell loss and alpha-cell expansion in patients with type 2 diabetes mellitus in Korea. *J Clin Endocrinol Metab* 2003; 88: 2300–2308.
  32. Wandell PE, Carlsson AC. Gender differences and time trends in incidence and prevalence of type 2 diabetes in Sweden—a model explaining the diabetes epidemic worldwide today? *Diabetes Res Clin Pract* 2014; 106: e90–e92.
  33. Gale EA, Gillespie KM. Diabetes and gender. *Diabetologia* 2001; 44: 3–15.
  34. Franconi F, Seghieri G, Canu S, *et al.* Are the available experimental models of type 2 diabetes appropriate for a gender perspective? *Pharmacol Res* 2008; 57: 6–18.
  35. Prasannarong M, Vichaiwong K, Saengsirisuwan V. Calorie restriction prevents the development of insulin resistance and impaired insulin signaling in skeletal muscle of ovariectomized rats. *Biochim Biophys Acta* 2012; 1822: 1051–1061.
  36. Sakata A, Mogi M, Iwanami J, *et al.* Female exhibited severe cognitive impairment in type 2 diabetes mellitus mice. *Life Sci* 2010; 86: 638–645.
  37. Bailey CJ, Ahmed-Sorour H. Role of ovarian hormones in the long-term control of glucose homeostasis. Effects of insulin secretion. *Diabetologia* 1980; 19: 475–481.
  38. Brelje TC, Bhagroo NV, Stout LE, *et al.* Prolactin and oleic acid synergistically stimulate beta-cell proliferation and growth in rat islets. *Islets* 2017; 9: e1330234.

## SUPPORTING INFORMATION

Additional supporting information may be found online in the Supporting Information section at the end of the article.

**Figure S1** | Glucose tolerance test in *ihs* mice at each weeks of age.

**Figure S2** | Non-fasting plasma insulin levels.

**Figure S3** | Plasma active GLP-1 levels after glucose oral administration.

**Figure S4** | Pancreatic islet morphology in aged male *ihs* mice.

**Figure S5** | Pancreatic islet morphology in female *ihs* mice.

**Figure S6** | Insulin secretion in the isolated islets of *ihs* mice.

**Table S1** | RT-qPCR primer sets of genes associated with monogenic diabetes.

**Appendix S1** | Mice.

**Appendix S2** | Non-fasting plasma insulin levels.

**Appendix S3** | Plasma active GLP-1 levels.

**Appendix S4** | Insulin secretion from the *in situ* perfused pancreas.

**Appendix S5** | Insulin secretion of islets isolated from *ihs* mice.

**Appendix S6** | Islet morphology analysis.

**Appendix S7** | RT-qPCR analysis.